

DISTRIBUTED ESTIMATION OF STATIC FIELDS IN WIRELESS SENSOR NETWORKS USING THE FINITE ELEMENT METHOD

Toon van Waterschoot and Geert Leus

Faculty of Electrical Engineering, Mathematics, and Computer Science (EEMCS)
Delft University of Technology (TU Delft), The Netherlands
E-mail: t.j.m.vanwaterschoot@tudelft.nl, g.j.t.leus@tudelft.nl

ABSTRACT

This paper deals with the distributed implementation of a recently proposed algorithm for the estimation of static fields. The algorithm combines wireless sensor network (WSN) field measurements with a physical field model in the form of a partial differential equation (PDE), such that the field can be estimated at locations different from the WSN sensor node locations. By discretizing the PDE using the finite element method (FEM), the physical field model reduces to a highly sparse linear system of equations. It is shown how this FEM-induced sparsity pattern can be exploited in the design of a distributed implementation such as to minimize the communication effort and data storage required in the WSN. Simulation results illustrate that a significant improvement in field estimation accuracy can be obtained, compared to the case when only WSN measurements (without a physical model) are used.

Index Terms— distributed estimation, wireless sensor networks, finite element method, convex optimization, sparsity

1. INTRODUCTION

Many physical phenomena are understood to be governed by a partial differential equation (PDE) that relates the spatiotemporal variation of a field to the underlying driving source function. The problem of field estimation is hence equivalent to the problem of solving a PDE subject to certain initial and/or boundary conditions. A particularly popular numerical method for solving such initial/boundary value problems is the finite element method (FEM), which has been extensively covered in literature, see, e.g., [1]. There are, however, two drawbacks when considering the FEM for field estimation: (1) the FEM is unsuitable for problems with limited or no knowledge about the driving source, and (2) the FEM approximation accuracy is linearly related to the resolution of the mesh (that is, the spatiotemporal domain discretization) [1, Th. 1.10], which implies that a high accuracy can only be attained at the cost of a high dimensionality.

The recent advent of wireless sensor networks (WSNs) offers a significantly different yet attractive approach to field estimation. Indeed, the dense deployment of sensor nodes inside a spatially distributed field makes it possible to collect a large number of local field estimates which can then be gathered in a fusion center for global field reconstruction. However, a fundamental issue with this approach is how to estimate field values at locations different from the WSN sensor node locations. A naive approach would be to interpolate the field values estimated at the sensor node locations to obtain field values at arbitrary locations, yet the choice of the interpolant

This work was supported by NWO-STW under the VICI program (project 10382).

will then carry an implicit assumption on the spatiotemporal variation of the field. A more rigorous approach is to combine the WSN field measurements with a PDE-based field model. In [2] and [3], the field estimation problem is recast in a dynamic state estimation problem, in which the state equation is derived from a discretization of the PDE (using the FEM [2] or the finite difference method (FDM) [3]) while only a subset of the states (i.e., the field values at the sensor node locations) is propagated to the measurement equation. However, these methods still require significant knowledge about the driving source: in [2] it is assumed that a noisy observation of the (continuous) source function is available, while in [3] the source function is assumed to be composed solely of point source contributions at locations where sensor nodes have been deployed. A different yet related problem that has recently been considered concerns the estimation of the (initial) driving source function from WSN field measurements. This inverse problem has been tackled in [4],[5] for the case of a source function composed of one or more point sources, by fitting the field measurements to a spatiotemporal discretization of the analytical PDE solution.

We have recently proposed a new framework for field estimation based on the combination of WSN field measurements with a physical model in the form of a PDE [6]. The field estimation problem is formulated as a constrained optimization problem, in which the constraints originate from a FEM discretization of the PDE and its initial and/or boundary conditions, and the objective minimizes the misfit between the estimated and measured field values at the sensor node locations. In contrast to the approaches in [2], [3], we do not assume the source function or the possible locations of point sources to be known, however, some prior knowledge on the nature of the field and/or source functions (such as sparsity or nonnegativity) needs to be included to avoid ending up with an underdetermined problem. In [6], a cooperative FEM-constrained field estimation (FCE) algorithm was proposed for static 2-D fields governed by a Poisson PDE, with applications in gravitation, electrostatics, fluid mechanics, and thermostatics, to name just a few. The cooperative FCE algorithm relies on the availability of a fusion center (FC) that collects the WSN field measurements and solves the optimization problem in a centralized manner. In this paper, we propose a distributed implementation of the FCE algorithm, in which each of the WSN nodes solves a sub-problem of the original optimization problem. The main contribution consists in the exploitation of the sparsity pattern that is introduced by the FEM discretization, such as to minimize the communication cost and data storage required in the WSN. Simulation results are included to illustrate that the distributed FEM-constrained field estimation (D-FCE) algorithm performs only slightly worse than the FC-based cooperative FCE algorithm, yet still outperforms an estimation algorithm based on WSN measurements only.

2. FEM-CONSTRAINED FIELD ESTIMATION

2.1. Problem Statement

Consider the 2-D Poisson PDE (with $\nabla = [\partial/\partial x, \partial/\partial y]$)

$$-\nabla^2 u(x, y) = s(x, y) \quad (1)$$

where the source function $s(x, y)$ and the field function $u(x, y)$ are infinite-dimensional functions of the spatial variables (x, y) defined on a 2-D domain $\Omega \subset \mathbb{R}^2$. The field $u(x, y)$ is measured using a WSN with sensor nodes at J discrete locations (x_j, y_j) , $j = 1, \dots, J$. Each of the J sensor nodes provides N field measurements (with $\mathbf{1}_{N \times 1} = [1 \dots 1]^T$),

$$\mathbf{v}_j = \begin{bmatrix} v_j^{(1)} \\ \vdots \\ v_j^{(N)} \end{bmatrix} = u(x_j, y_j) \mathbf{1}_{N \times 1} + \begin{bmatrix} w_j^{(1)} \\ \vdots \\ w_j^{(N)} \end{bmatrix}, \quad j = 1, \dots, J \quad (2)$$

which are obtained by sensing the field at successive time instants and/or equipping the WSN nodes with multiple sensors. The measurement noise $w_j^{(n)}$ at the j th sensor node is assumed to be i.i.d. with variance σ_j^2 , and independent of the measurement noise at other sensor nodes. Additionally, the field may be subject to boundary conditions of the Dirichlet or Neumann type. Since the boundary conditions appear as additional (and known) terms on the right-hand side of the FEM system of equations [1, Ch. 1], we can assume zero boundary conditions without loss of generality to simplify notation.

Our aim is to estimate the field $u(x, y)$ at $J + P$ distinct locations, without assuming knowledge of the source function $s(x, y)$. These locations include the J sensor node locations (x_j, y_j) , $j = 1, \dots, J$ as well as the locations (x_{J+p}, y_{J+p}) , $p = 1, \dots, P$ of P points of interest (POIs) at which no sensors have been deployed.

2.2. Finite Element Method

In a nutshell, the FEM reduces a boundary value problem to a square system of linear equations in a four-step procedure [1]: (1) converting the boundary value problem to its weak formulation, (2) performing integration by parts to relax the differentiability requirements, (3) approximating the infinite-dimensional field and source functions in a finite-dimensional subspace, and (4) enforcing the field approximation error to be orthogonal to this subspace.

The subspace approximation of the field and source functions $u(x, y)$ and $s(x, y)$ is defined as

$$\tilde{u}(x, y) = \sum_{k=1}^{K_\Omega} u_k \phi_k(x, y), \quad \tilde{s}(x, y) = \sum_{k=1}^{K_\Omega} s_k \phi_k(x, y). \quad (3)$$

where K_Ω denotes the subspace order, $\phi_k(x, y)$, $k = 1, \dots, K_\Omega$ is a subspace basis, and $\{u_k, s_k\}$, $k = 1, \dots, K_\Omega$ represent the basis expansion coefficients. The square system of linear equations obtained in the FEM, also known as the Galerkin equations, is then given by

$$\mathbf{A}\mathbf{u} = \mathbf{B}\mathbf{s} \quad (4)$$

where the so-called stiffness and mass matrices are defined by

$$[\mathbf{A}]_{ij} = \int_{\Omega} \nabla \phi_j(x, y) \cdot \nabla \phi_i(x, y) dx dy \quad (5)$$

$$[\mathbf{B}]_{ij} = \int_{\Omega} \phi_j(x, y) \phi_i(x, y) dx dy \quad (6)$$

and the field and source vectors contain the corresponding basis expansion coefficients, i.e.,

$$\mathbf{u} = [u_1 \quad \dots \quad u_{K_\Omega}]^T, \quad \mathbf{s} = [s_1 \quad \dots \quad s_{K_\Omega}]^T. \quad (7)$$

The FEM basis functions are often chosen to be piecewise linear functions possessing two particular properties. First of all, by ensuring that $\phi_i(x_k, y_k) = \delta(i - k)$, $i = 1, \dots, K_\Omega$ at exactly K_Ω locations (x_k, y_k) , $k = 1, \dots, K_\Omega$, the basis expansion coefficients in the FEM subspace approximation are equal to the field/source values at these locations, i.e., $u_k = u(x_k, y_k)$, $s_k = s(x_k, y_k)$. The FEM thus provides a spatial sampling of the field and source functions. Second, the basis functions are chosen to have small spatial support, in the sense that the k th basis function is non-zero only in a limited area around the location (x_k, y_k) . Consequently, the stiffness and mass matrices defined in (5) and (6) have a highly sparse structure, which will be exploited when deriving a distributed implementation in Section 3. The choice of the points (x_k, y_k) , $k = 1, \dots, K_\Omega$, referred to as the FEM nodes, is of particular importance, since these should include (1) the sensor node and POI locations and (2) a sufficiently large number of ‘‘free’’ points such that a high-quality mesh (and consequently a well-conditioned system of Galerkin equations) can be obtained. An example scenario (discussed in detail in Section 4) with $J = 20$ sensor nodes, $P = 20$ POIs, and $K_\Omega = 166$ FEM nodes is shown in Fig. 1(a). Finally, we should note that the dimension of the Galerkin system of equations can be reduced from K_Ω to K (which corresponds to the number of interior nodes in the mesh) by eliminating the boundary conditions.

We refer to [1] for a more profound treatment of the FEM, and to [7] for an introduction to mesh generation.

2.3. FEM-Constrained Cooperative Field Estimation

The WSN measurement model in (2) and the FEM system of equations in (4) can be combined into a single estimation problem by minimizing the sum of squared WSN measurement errors subject to the Galerkin equations [6],

$$\min_{\mathbf{u}, \mathbf{s}} \sum_{j=1}^J \|\mathbf{v}_j - u_j \mathbf{1}_{N \times 1}\|_2^2 \quad \text{s. t.} \quad \mathbf{A}\mathbf{u} = \mathbf{B}\mathbf{s} \quad (8)$$

However, this optimization problem is heavily underdetermined, which requires the inclusion of additional objective functions or constraints. In many signal processing applications, it makes sense to assume that the source function $s(x, y)$ is composed solely of point source contributions (which is indeed an assumption that is also exploited in [3]-[5]). This assumption naturally leads to the inclusion of a sparsity-inducing regularization term on the source vector \mathbf{s} , since the dimension K of the Galerkin system of equations will typically be much larger than the number of point sources. Moreover, a static point source is inherently positive-valued (otherwise it would be a sink), and consequently the Poisson PDE generates a nonnegative field if the boundary conditions are also nonnegative. Appending a sparsity-inducing regularization term and appropriate nonnegativity constraints to the optimization problem (8), results in the following constrained optimization problem,

$$\min_{\mathbf{u}, \mathbf{s}} \sum_{j=1}^J \|\mathbf{v}_j - u_j \mathbf{1}_{N \times 1}\|_2^2 + \lambda \|\mathbf{s}\|_1 \quad (9)$$

$$\text{s. t.} \quad \mathbf{A}\mathbf{u} = \mathbf{B}\mathbf{s}, \quad \mathbf{u} \geq \mathbf{0}_{K \times 1}, \quad \mathbf{s} \geq \mathbf{0}_{K \times 1} \quad (10)$$

This is a convex problem, which can be readily solved using convex optimization software such as CVX [8].

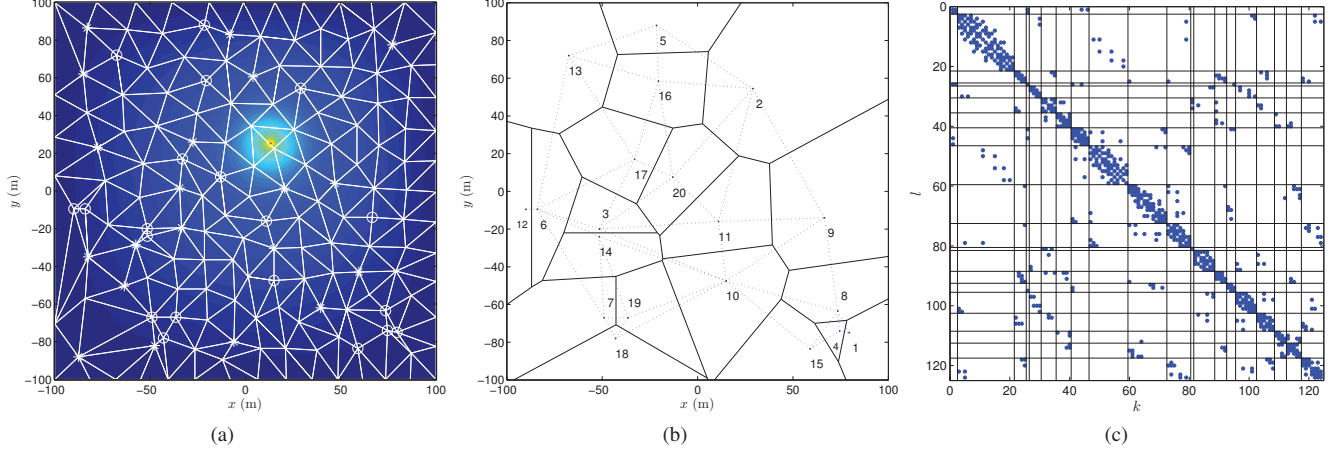


Fig. 1. Example scenario: (a) field contour plot with FEM mesh generated for 20 randomly deployed WSN nodes (o) and POIs (*), (b) cluster boundaries (–) and required WSN communication links (–.-), (c) partitioning and sparsity pattern of stiffness and mass matrices.

3. DISTRIBUTED FCE IMPLEMENTATION

3.1. Clustering of FEM Nodes

In the distributed case, we envisage that every WSN node estimates *part* of the field and source vectors. A first step towards a distributed implementation is thus to decide which WSN node will estimate which coefficients of \mathbf{u} and \mathbf{s} . This requires a clustering of the K FEM nodes into J clusters. We employ a simple clustering approach in which each FEM node is assigned to the cluster of the closest WSN node. In this way, the clusters are defined by a 2-D Voronoi tessellation of the WSN nodes. Fig. 1(b) shows the resulting cluster boundaries for the example scenario depicted in Fig. 1(a).

The clustering naturally leads to a partitioning of the unknown field and source vectors,

$$\mathbf{u} = [\mathbf{u}_1^T \ \dots \ \mathbf{u}_J^T]^T, \quad \mathbf{s} = [\mathbf{s}_1^T \ \dots \ \mathbf{s}_J^T]^T \quad (11)$$

where we have assumed that the field and source coefficients in \mathbf{u} and \mathbf{s} are ordered clusterwise by an appropriate row permutation. We use K_j to denote the number of FEM nodes in the j th cluster.

3.2. Separability of FCE Problem

Given the partitioning of the unknown field and source vectors in (11), we can divide the constrained optimization problem (9)-(10) into J subproblems, each of which is solved in one WSN node. The sum of squared WSN measurement errors and the sparsity-inducing regularization term in (9), as well as the nonnegativity constraints in (10) are fully separable. On the other hand, the Galerkin equality constraints in (10) are only partially separable, and hence the main challenge is to separate these constraints in a way that requires a minimal communication effort and data storage in the WSN.

Assuming that the equations and variables in the Galerkin system have been ordered clusterwise by appropriate row and column permutations, the stiffness and mass matrices can be partitioned into blocks $\mathbf{A}_{ji}, \mathbf{B}_{ji}$ of size $K_j \times K_i$. The sparsity pattern of these partitioned matrices is shown in Fig. 1(c) for the example WSN scenario depicted in Fig. 1(a), and can be formalized as follows. First, let us define $\mathcal{N}_C(j) \subset \{1, \dots, J\}$ as the set of indices of clusters that are neighboring the j th cluster. Then all blocks $\mathbf{A}_{ji}, \mathbf{B}_{ji}$ with $i \notin \mathcal{N}_C(j)$ are $K_j \times K_i$ zero matrices. Second, let $\mathcal{N}_N(k) \subset \{1, \dots, K\}$ denote the set of indices of nodes that are directly connected to the k th node in the FEM mesh. Then the coefficients

a_{kl}, b_{kl} with $l \notin \mathcal{N}_N(k)$ are equal to zero. It can be observed from Fig. 1(c) that $\mathcal{N}_N(k)$ primarily consists of indices of nodes that are in the same cluster as the k th node, i.e., the off-diagonal blocks in \mathbf{A} and \mathbf{B} are much more sparse than the diagonal blocks.

In each of the J subproblems, we will therefore only consider a subset of the Galerkin equality constraints, corresponding to the j th block row of \mathbf{A} and \mathbf{B} . By exploiting the above sparsity pattern, these equality constraints can be written as

$$\mathbf{A}_{jj}\mathbf{u}_j - \mathbf{B}_{jj}\mathbf{s}_j = \sum_{i \in \mathcal{N}_C(j)} \mathbf{c}_{ji} \quad \text{with} \quad \mathbf{c}_{ji} \triangleq \mathbf{B}_{ji}\mathbf{s}_i - \mathbf{A}_{ji}\mathbf{u}_i \quad (12)$$

Three important remarks are in place here. First, the calculation of the vectors \mathbf{c}_{ji} is performed in WSN node i , and so the j th WSN node only needs to store the blocks $\mathbf{A}_{ij}, \mathbf{B}_{ij}$ for $i = j$ and $i \in \mathcal{N}_C(j)$ in its memory, instead of the full matrices \mathbf{A}, \mathbf{B} . Second, it can be seen that the j th WSN node only needs to communicate the vectors \mathbf{c}_{ij} to the WSN nodes of neighboring clusters, while the actual field and source blocks \mathbf{u}_j and \mathbf{s}_j need not be shared. This is advantageous in terms of communication cost, since \mathbf{c}_{ij} is sparse and only its non-zero entries need to be shared (the positions of which are known in node i from the structure of \mathbf{A}_{ji}). The required communication links are shown for the example scenario in Fig. 1(b). Third, by only considering the constraints (12) in the j th subproblem, some equality constraints from the original problem (9)-(10) are ignored when estimating $\mathbf{u}_j, \mathbf{s}_j$, which may decrease the field estimation accuracy. While the inclusion of these ignored constraints would be feasible by using the same approach as in (12), i.e., moving terms involving $\mathbf{u}_i, \mathbf{s}_i$, $i \neq j$ to the right hand side, the communication requirements would be significantly increased.

3.3. Distributed FCE Algorithm

Given the separability of the FCE problem discussed above, a distributed FCE algorithm can be derived by applying a block coordinate descent method [9] to the estimation of the partitioned field and source vectors. The resulting iterative algorithm is summarized in Algorithm 1, and typically requires about $L = 5$ iterations to converge. The vectors γ_{ji} , containing the non-zero entries of \mathbf{c}_{ji} , can either be initialized to zero (cold start) or by performing a pre-iteration in which each WSN node shares its measurement average with nodes in neighboring clusters (warm start).

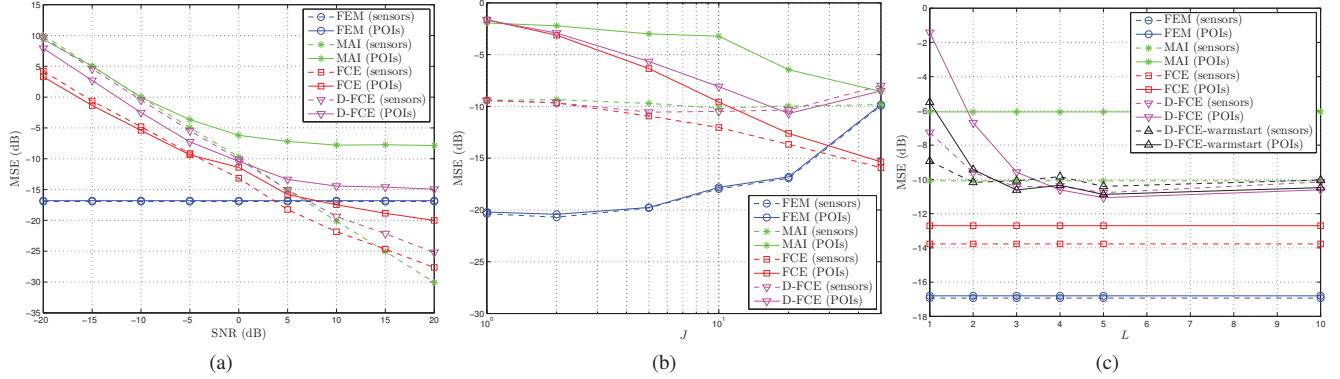


Fig. 2. Comparison of field estimation MSE at sensor node locations (- -) and POI locations (-) for different estimation algorithms, plotted vs. (a) SNR of WSN measurements, (b) number of WSN nodes J , (c) number of iterations L in the distributed D-FCE implementation.

4. SIMULATION RESULTS

We simulate a static 2-D field governed by the Poisson PDE on a square domain of 200 x 200 m, with zero boundary conditions. The field is driven by a single point source with coordinates (13, 25) m and unit amplitude. A WSN with $J = 20$ sensor nodes is randomly deployed in a square area of 180 x 180 m, maintaining a margin of 20 m to the domain boundary with the aim of avoiding ill-shaped boundary elements. Similarly, $P = 20$ POIs are randomly chosen in the area where the WSN sensor nodes are located. Each WSN sensor node provides $N = 10$ field measurements, corrupted by i.i.d. measurement noise with a variance that yields a local 0 dB signal-to-noise ratio (SNR). The mesh generation algorithm [7] is initialized by appending a set of equally spaced nodes at a mutual distance of $h_0 = 20$ m to the fixed subset of FEM nodes consisting of the sensor nodes, POIs, and domain corners.

Two benchmark algorithms are evaluated for comparison with the proposed algorithm: a FEM with *known* source vector that does not employ WSN measurements, and a measurement averaging and interpolation (MAI) method that produces local field estimates by measurement averaging at the WSN sensor nodes and linear interpolation at the POIs. The algorithms are compared in terms of the mean squared relative field estimation error (MSE) at the sensor nodes and at the POIs, which is calculated by averaging the squared relative error over $N_{MC} = 100$ Monte Carlo trials [6].

Fig. 2 displays the MSE behavior when one of the simulation parameters is varied while the other parameters are kept fixed at the values given earlier. A first observation is that there is a small but consistent performance decrease when replacing the FC-based cooperative FCE algorithm proposed in [6] with its distributed implementation presented here. This can be explained by the fact that only a subset of the Galerkin equality constraints is imposed to each of the J subproblems. The number of equality constraints that are thus ignored increases as the cluster dimensions K_j decrease, which is indeed observed in Fig. 2(b) for large values of J . A second observation is that the proposed D-FCE algorithm significantly outperforms the MAI algorithm at the POI locations, which confirms our intuition that the use of a physical model indeed offers a decent alternative to “naive” field interpolation at POIs. A third and final observation is that the “warm start” procedure explained in Section 3.3 may effectively reduce the number of iterations required for convergence of the D-FCE algorithm.

Algorithm 1 Distributed FEM-Constrained Field Estimation

Input Initial γ_{ji} , $j \in \{1, \dots, J\}$, $i \in \mathcal{N}_C(j)$

Output Field and source vector estimates $\mathbf{u}_j, \mathbf{s}_j$, $j \in \{1, \dots, J\}$

- 1: **for** $l = 1, \dots, L$ **do**
- 2: **for** $j = 1, \dots, J$ **do**
- 3: $\forall i \in \mathcal{N}_C(j)$: Reconstruct $\mathbf{c}_{ji} = \mathbf{B}_{ji}\mathbf{s}_i - \mathbf{A}_{ji}\mathbf{u}_i$ from γ_{ji}
- 4: Solve $\min_{\mathbf{u}_j, \mathbf{s}_j} \|\mathbf{v}_j - \mathbf{u}_j \mathbf{1}_{N \times 1}\|_2^2 + \lambda \|\mathbf{s}_j\|_1$ subject to $\mathbf{A}_{jj}\mathbf{u}_j - \mathbf{B}_{jj}\mathbf{s}_j = \sum_{i \in \mathcal{N}_C(j)} \mathbf{c}_{ji}$, $\mathbf{u}_j, \mathbf{s}_j \geq \mathbf{0}_{K_j \times 1}$
- 5: $\forall i \in \mathcal{N}_C(j)$: Calculate $\mathbf{c}_{ij} = \mathbf{B}_{ij}\mathbf{s}_j - \mathbf{A}_{ij}\mathbf{u}_j$
- 6: $\forall i \in \mathcal{N}_C(j)$: Collect the non-zero entries of \mathbf{c}_{ij} in γ_{ij}
- 7: $\forall i \in \mathcal{N}_C(j)$: Transmit γ_{ij} to WSN node i
- 8: **end for**
- 9: **end for**

5. REFERENCES

- [1] S. C. Brenner and L. R. Scott, *The mathematical theory of finite element methods*, Springer, New York, 2008.
- [2] F. Sawo, K. Roberts, and U. D. Hanebeck, “Bayesian estimation of distributed phenomena using discretized representations of partial differential equations,” in *Proc. 3rd Int. Conf. Informat. Control Autom. Robot. (ICINCO '06)*, Setubal, Portugal, Aug. 2006, pp. 16–23.
- [3] H. Zhang et al., “Dynamic field estimation using wireless sensor networks: Tradeoffs between estimation error and communication cost,” *IEEE Trans. Signal Process.*, vol. 57, no. 6, pp. 2383–2395, June 2009.
- [4] T. Zhao and A. Nehorai, “Distributed sequential Bayesian estimation of a diffusive source in wireless sensor networks,” *IEEE Trans. Signal Process.*, vol. 55, no. 4, pp. 1511–1524, Apr. 2007.
- [5] J. Ranieri, A. Chebira, Y. M. Lu, and M. Vetterli, “Sampling and reconstructing diffusive fields with localized sources,” in *Proc. 2011 IEEE Int. Conf. Acoust., Speech, Signal Process. (ICASSP '11)*, Prague, Czech Republic, May 2011, pp. 4016–4019.
- [6] T. van Waterschoot and G. Leus, “Static field estimation using a wireless sensor network based on the finite element method,” in *Proc. Int. Workshop Comput. Adv. Multi-Sensor Adaptive Process. (CAMSAP '11)*, San Juan, PR, USA, to appear, Dec. 2011.
- [7] P.-O. Persson and G. Strang, “A simple mesh generator in MATLAB,” *SIAM Review*, vol. 46, no. 2, pp. 329–345, June 2004.
- [8] M. Grant and S. Boyd, “CVX: Matlab software for disciplined convex programming, v. 1.21,” <http://cvxr.com>, Apr. 2011.
- [9] P. Tseng, “Convergence of a block coordinate descent method for non-differentiable minimization,” *J. Optimiz. Theory App.*, vol. 109, no. 3, pp. 475–494, June 2001.